FISHERIES OCEANOGRAPHY

FISHERIES OCEANOGRAPHY Fish. Oceanogr. 22:2, 90–101, 2013

Variation in DVM behaviour of juvenile and adult pearlside (*Maurolicus muelleri*) linked to feeding strategies and related predation risk

ARVED STABY,[1,2,*] JANTRA SRISOMWONG[3] AND RUNE ROSLAND[1]

[1]*Department of Biology, University of Bergen, P O Box 7803, 5020 Bergen, Norway*
[3]*Kasetsart University, 50 Ngam Wong Wan Road, Ladyaow Chatuchak, 10900 Bangkok, Thailand*

ABSTRACT

In the Norwegian fjord Masfjorden, different developmental stages of the mesopelagic planktivore *Maurolicus muelleri* form vertically separate sound scattering layers (SSLs) and in late autumn display different diel vertical migration (DVM) behaviour. Post-larvae and juvenile fish perform normal crepuscular DVM, whereas the large majority of adults remain at depth throughout the diel period. In this study we examined the stomach contents of juvenile and adult fish caught at different times and depths during a 24-h period in autumn. The different DVM behaviour of these two SSLs in addition to a shallow layer believed to be composed of post-larvae is explained with a model for visual foraging in aquatic environments that uses gradients in vertical light intensity and copepod density and size as input variables. Field data revealed that vertically migrating juveniles distributed at a higher ambient light intensity and on average consumed 25 times more copepods than non-migrating adult fish. The model showed that juveniles experienced a 15 times higher prey encounter rate and a higher level of predation risk than non-migrating adults, and that the energetic benefits for post larvae and juveniles from prolonged feeding in a nearly constant and brighter environment outweigh the associated predation risk. The model also suggests that the visual detection range of piscivore predators is relatively more limited by the turbid surface water than that of their prey, which provide the post-larva and juvenile life-stages of *M. muelleri* a window of reduced visual predation near the surface.

Key words: diel vertical migration, feeding strategy, ontogenetic variation, predation risk, sound scattering layers, trade-off

INTRODUCTION

The mesopelagic planktivore fish Mueller's pearlside (*Maurolicus muelleri*) is a circumglobal species that is also abundant in fjordic environments (Gjøsæter and Kawaguchi, 1980; Parin and Kobyliansky, 1996). In Norwegian fjords the mesopelagic micronekton community above 200 m depth is typically dominated by the pearlside (Giske *et al.*, 1990; Goodson *et al.*, 1995; Kaartvedt *et al.*, 2008; Staby *et al.*, 2011). Different ontogenetic stages of the species form vertically separate sound scattering layers (SSLs), which typically perform diel vertical migrations (DVM), reaching the surface layer at dusk and descending back to deeper day depths at dawn (Baliño and Aksnes, 1993; Staby *et al.*, 2011). However, continuous acoustic observations of pearlside SSLs revealed that adult fish, constituting the deepest SSL, do not perform DVM between late autumn and early spring, whereas younger life stages, forming shallower SSLs, display DVM during the same period (Staby *et al.*, 2011).

DVM is a common behaviour of a range of aquatic organisms (Neilson and Perry, 1990; Cohen and Forward, 2009). The hypothesized adaptive value of DVMs is (i) to minimize predation mortality through predator avoidance (Eggers, 1978; Hrabik *et al.*, 2006) by maintaining a light environment with a reduced predation risk, referred to as the anti-predation window, which allows continued foraging (Clark and Levy, 1988; Scheuerell and Schindler, 2003), (ii) to maximize growth by distributing at optimal temperatures (Wurtsbaugh and Neverman, 1988; or (iii) to improve feeding conditions by distributing at depth ranges of prey organisms (Neilson and Perry, 1990).

*Correspondence. e-mail: arved.staby@imr.no
[2]Present address: Institute of Marine Research P.O. Box 1870 N 5817 Bergen Norway.
Received 25 September 2011
Revised version accepted 24 September 2012

 doi:10.1111/fog.12012

Previous studies suggest that pearlside feed visually during light hours and that foraging depth and diet composition may vary seasonally (Rasmussen and Giske, 1994; Bjelland, 1995; Bagøien *et al.*, 2001). The dominating prey are copepods in autumn/winter (Giske *et al.*, 1990; Bagøien *et al.*, 2001), copepods and diatoms in early spring (Bjelland, 1995) and cladocerans, bivalve veligers and copepods in late spring (Rasmussen and Giske, 1994).

An increase in ambient light intensity may improve feeding conditions as a result of an increased prey detection rate (Ryer and Olla, 1999; Vogel and Beauchamp, 1999). However, successful prey detection is also related to water clarity, i.e., to the degree of turbidity (Utne-Palm, 2002). For larger piscivores that have a long detection range, an increase in turbidity will be more disruptive than for smaller planktivorous fish with a shorter detection distance (Giske *et al.*, 1994).

In Masfjorden, pearlside are heavily preyed on by the visually feeding gadoid fish species blue whiting (*Micromesistious potassou*), saithe (*Pollachius virens*), haddock (*Melanogrammus aeglefinus*) and pollack (*Pollachius pollachius*; Giske *et al.*, 1990; Rasmussen and Giske, 1994; Bjelland, 1995). Based on the distribution of acoustic echoes, large piscivorous fish occur throughout the water column in Masfjorden, where in winter their densities ranged from 2.5 to 12 ind $(10^6\ m^3)^{-1}$ (Giske *et al.*, 1990).

In a plain pelagic environment where the risk for small planktivores to be preyed on by larger visually foraging piscivores increases with increasing light intensity, planktivores reduce their conspicuousness through transparency, silvering and counter illumination (Widder, 1999; Warrant and Locket, 2004). The camouflaging efficiency of transparency and silvering seems to depend on ambient scattering properties and light intensity, i.e., transparency appears to be more effective than silvering at shallower depths under brighter conditions and pronounced horizontal scattering (Johnsen and Sosik, 2003).

Selecting a brighter environment thus involves the trade-off between gaining energy (growth) and predation risk (Lima and Dill, 1990; De Robertis, 2002). Whether an individual will choose to improve its fitness by foraging rather than reducing predation risk or vice versa may depend on its ontogeny (size), its current energetic state, and the potential for future reproduction and growth (Giske and Aksnes, 1992; Houston *et al.*, 1993; Rosland, 1997; Grand, 1999).

In this study we attempt to explain acoustically observed differences in diel vertical migration behaviour of vertically separate ontogenetic stages by using a model for visual foraging in aquatic environments (Aksnes and Utne, 1997), in combination with data on stomach contents of pearlside and vertical structures in environmental variables. Specifically we (i) calculate how feeding and predation rates of different pearlside length groups – post-larvae, juveniles and adults – are potentially influenced by vertical gradients in light intensity, water turbidity, zooplankton abundance and zooplankton size throughout the different depth-time trajectories of the SSLs in Masfjorden, and (ii) discuss the DVM strategies of different length groups in relation to ontogenetically driven trade-offs between growth and survival and the effects of fish size on visual foraging and predation processes.

MATERIALS AND METHODS

Study location

Biological and environmental data were collected in Masfjorden on the west coast of Norway (60°50′N, 5°30′E) on 2 and 3 November 2007 with the RV *Håkon Mosby*, University of Bergen. The fjord is roughly 20 km long and on average 1 km wide, with a sill depth of 75 m and a maximum depth of 494 m (Fig. 1).

Data collection and analysis

Continuous acoustic recordings were made with an upward-facing 38-kHz (SIMRAD) split beam echo sounder placed on the fjord bottom at 390 m depth (Kaartvedt *et al.*, 2009). An echogram for 2 November was generated in MATLAB (Mathworks). The depth of the upper and lower sound scattering layer (SSL) edge was determined by obtaining the average acoustic volume back scattering (Sv) for every 1 m vertical and 10 min horizontal bin, and then establishing the depth where the Sv dropped below -75 dB m^{-1}.

Vertical temperature measurements were obtained with a SEABIRD 911 CTD. Surface irradiance (photosynthetically active radiation, 400–700 nm) was measured during the diel cycle with a calibrated LI-190 quantum sensor (Li-Cor Biosciences). The sensor was mounted on top of the bridge of the RV *Håkon Mosby*, and recorded data was stored on a Li-1400 data logger at 5-min intervals. Light intensity I_d at depth d was calculated at 1-m intervals from the surface to 200 m depth:

$$I_d = I_{d-1} \exp(-K_d D_d) \quad (1)$$

where D_d is distance and K_d average light attenuation coefficient between depth d and $d–1$.

The light attenuation coefficient was estimated from proxies (salinity, dissolved oxygen, Chl-*a*) using

Figure 1. Masfjorden on the west coast of Norway. Biological data were collected within the rectangle. Environmental and multinet stations are shown as solid circles, and the position of the acoustic transducer is indicated by the triangle.

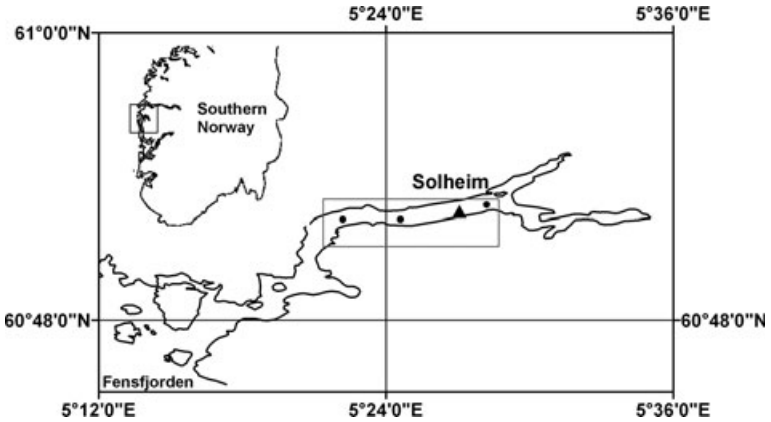

a regression model (Aksnes *et al.*, 2009) based on data from the same fjord. The regression model was established on data sampled between 29 October and 5 November 2006, when Chl-*a* concentrations are usually low. We applied the regression model on CTD-data sampled 1 November 2007 by assuming the model produces valid estimates of light absorption for our purposes.

The species composition of SSLs is presented and discussed in Staby *et al.* (2011) and was determined with pelagic Harstad trawls equipped with a multisampler unit that included three remotely controllable cod ends with 20-mm mesh size (Engås *et al.*, 1997). Trawling duration was generally 10 min at a speed of 3 knots, and the trawl depth was monitored with a depth sensor. A sub-sample of pearlside (if possible, at least 100 fish) was taken from each trawl catch and frozen for later stomach content analysis. We combined all biological data from subsequent tows that fished at similar depths and within a short time window (20–40 min) to increase the sample size for some of the stations (Table 1, Stations 1 and 2).

Depending on sub-sample size, 40 frozen fish were randomly selected from the frozen fish collected onboard the research vessel. Fish were thawed and excess moisture removed with absorbent paper before measuring standard length (nearest mm) and weight (nearest mg). The weight (W) – length (L) relationship constants a and b were estimated by regression analysis for juvenile and adult fish combined ($W = 0.0082\ L^{3.18}$).

Pearlside stomachs were dissected out and the contents spread out on a petri dish and inspected under a stereo or light microscope. A total of 423 stomachs were analysed. The degree of stomach fullness was measured on a scale of 0–1, where 0 = empty, 0.25 = some content, 0.5 = half stomach, 0.75 = more than half full, and 1 = full stomach. Individual food items were identified to group level and counted. The degree of digestion was measured on a scale of 0–1, where 0 = fresh, 0.25 = digestion start, 0.5 = partly digested, 0.75 = unidentified and 1 = digested.

On four occasions, multinet (Hydro-Bios, Kiel) tows sampled zooplankton in 50-m depth bins between the surface and 450 m depth. The multinet has a 0.5 × 0.5 m opening with five nets (mesh size 180 μm) that can be closed remotely. Each net sample was divided into two subsamples using a Folsom

Table 1. Trawl station summary and number of fish examined for stomach content. Station numbers refer to numbers shown in Figure 2c.

Date	Station	Trawl No.	Trawl start time	Fishing depth (m)	Total fish analysed	% Empty stomachs
2 November 2007	1	158–160	00:28–00:59	35–42	43	42
	2	162–163	02:05–02:25	72–77	30	73
	3	164–165	03:19–03:52	156–162	120	94
	4	167–168	10:39–11:00	70–74	72	1
	5	170–171	12:13–12:34	135–136	80	43
3 November 2007	6	185–186	03:36–03:57	35	79	78

plankton splitter. One sample was frozen for ash-free dry weight (W_z) determination and the other sample was preserved in 70% alcohol solution. Plankton samples from each sampling interval were dried at 60°C for 24 h, weighed (dry weight), ashed at 490°C for 3 h, and weighed again (ash weight). W_z was obtained by subtracting the ash weight from the dry weight and multiplying the difference by a factor of two, since multinet samples were split into two subsamples. The sample in alcohol was used to estimate the number of zooplankton and to calculate the zooplankton density (N_d) in each sampling bin. The zooplankton radius at depth (R_d) of individual zooplankton was estimated from wet body mass by assuming that zooplankton has a spherical body shape and a density similar to water ($\sim$ 1 g cm^{-3}). Wet mass was calculated from W_z by multiplying by a factor of 14 (Giske *et al.*, 1990). A continuous vertical profile of the zooplankton variables was created by linear interpolation between the center (25, 75, …, 225 m) of the zooplankton sampling intervals, except between the surface and 25 m, which was assigned the value of the upper sampling interval.

Zooplankton encounters and mortality rate

Zooplankton encounter rate (E_N) and mortality rate of *M. muelleri* (M) due to visual predation were calculated by a model for visual range (V) in water (Aksnes and Utne, 1997). Model variables and parameters are shown in Table 2.

$$V^2 = I_d \exp(-B_d V)|C|\pi R_d^2 I_{\max} \frac{I_d}{k_I + I_d} \Delta T^{-1} \qquad (2)$$

where the visual range is a function of ambient light intensity (I_d), beam attenuation (B_d), inherent contrast of the prey against background (C), prey radius (R_d), the light-processing capacity at the retina (I_{max}), the half saturation coefficient for light entering the eye lens (k_I) and the light sensitivity threshold of the eye (ΔT). Visual range is approached by Newton–Rapson iterations of Eqn (2). The eye sensitivity threshold scales inversely to fish length according to:

$$\Delta T = k_T L^{-2} \qquad (3)$$

which implies that visual range increases proportionally to fish length. The scaling constant (k_T) was tuned to get zooplankton encounter in SSL3 within the range of the observed stomach contents. The visual range (V) of the fish is used to calculate its encounter rate with zooplankton individuals:

$$E_N = \pi(V \sin\theta)^2 \cdot v \cdot N_d \qquad (4)$$

where θ is the visual field angle, v is the swimming speed of the fish (one fish length per second) and N_d is zooplankton density at SSL depth d. Individual zooplankton mass (AFDW) at each depth and average fish

Table 2. Parameters and variables (capital letters) used in the text.

Symbol	Value	Unit	Explanation
B_d	$3K_d$	m^{-1}	Beam attenuation coefficient
D_d		m	Length of depth interval d
E_N		ind m^{-3} s^{-1}	Zooplankton encounter rate
E_W		g g^{-1} h^{-1}	Mass specific zooplankton encounter rate
I_d	–	μE m^{-2} s^{-1}	Light intensity at depth d
I_{max}		μE m^{-2} s^{-1}	Maximum light processing rate at retina
K_d		m^{-1}	Average light attenuation in depth interval d
L		m	Standard length of *M. muelleri*
N_d		ind m^{-3}	Zooplankton density at depth d
R_d		m	Zooplankton radius at depth d
ΔT		m^2	Visual sensitivity threshold
V		m	Visual range of fish
W		g	Wet mass of *M. muelleri*
W_F		g	AFDW of *M. muelleri* (20% of wet mass)
W_Z		g	AFDW of zooplankton
θ	30	degrees	Visual field angle of fish
C	0.5	–	Inherent contrast of prey (Zooplankton and *M. muelleri*)
k_I		μE m^{-2} s^{-1}	Half saturation for light at eye lens
k_M	5.7e-8	s^{-1}	Scaling constant for predation rate (Gjøsæter, 1981)
k_T	5×10^{-5}	–	Eye sensitivity parameter
v		m s^{-1}	Swimming speed of *M. muelleri* (one fish length s^{-1})

mass (AFDW) at each SSL were used to convert encounter rates (E_N in Eqn 4) to weight-specific (g zooplankton g fish^{-1} s^{-1}) equivalents:

$$E_W = \frac{E_N \cdot W_Z}{W_F} \quad (5)$$

The susceptibility of M. *muelleri* to visual predation is a function of the visual range of piscivore fish:

$$M = V^2 k_M \quad (6)$$

The visual range (V) of a visual predator is calculated from Eqn. (2) by substituting prey radius with half the body length of M. *muelleri*. The daily mortality constant (k_M) was calculated from the annual mortality of pearlside (Gjøsæter, 1981). However, the exact values of predation rate and the visual sensitivity threshold are not of great importance here as we are mostly interested in the relative differences between prey encounter and visual predation rates of M. *muelleri* during daytime and between depths. The different eye sensitivity threshold and larger prey radius enables a piscivore predator to detect M. *muelleri* at greater distances than M. *muelleri* can detect zooplankton. For the same reason the visual detection range of piscivore fish is relatively more inhibited by turbid water conditions and scattering light compared with M. *muelleri*.

Sensitivity analysis

To test the robustness of the model outputs with respect to model parameters and environmental variables we conducted a sensitivity analysis similar to Wei *et al*. (2004), where the sensitivity (*S*) measures changes in model output variables (M) relative to changes in parameter values (*p*) according to:

$$S = \left(\frac{M_x - M_0}{M_0}\right) \Big/ \left(\frac{p_x - p_0}{p_0}\right) \quad (7)$$

M_0 and p_0 are respectively the model output and parameter value in the standard simulation, and M_x and P_x the model output and parameter values in the sensitivity test. Wei *et al*. (2004) classified the sensitivity index as: Insensitive ($S < 0.1$), Sensitive ($0.1 < S < 0.4$) and More sensitive ($S > 0.4$). A negative value reflects an inverse model response to the parameter. The daily weight-specific prey encounter rate (E_w in Eqn. 5) and visual mortality rate (M in Eqn. 6) were used as model output variables (M) and the parameters and environmental variables tested are listed in Table 3. It was of particular interest to test whether the predicted relative differences between the SSLs remained under different parameter settings.

RESULTS

Environment

Sunrise was at 07:04 (UTC) and sunset at 15:40 h (UTC). Surface irradiance had a normal day pattern with a noon maximum around 174 μE, but with some irregularities in magnitude possibly due to fluctuations in cloud cover during the daytime (Fig. 2a).

Table 3. Sensitivity analysis of model 'parameters and variables' (see Table 2) and the 'factor' changed from standard run. The sensitivity index (*S*, Eqn. 7) for the model output variables 'Prey encounter' and 'Visual mortality rate' are displayed for each SSL.

		Prey encounter rate (E_w)			Visual mortality rate (M)		
Parameters and variables	Factor	SSL1	SSL2	SSL3	SSL1	SSL2	SSL3
C (zooplankton)	1.5	1.00	1.00	1.00			
	0.5	1.00	1.00	1.00			
ΔT (*M. muelleri*)	1.5	−0.67	−0.67	−0.67			
	0.5	−1.99	−1.99	−1.99			
k_I (*M. muelleri*)	1.5	−0.57	−0.62	−0.66	−0.54	−0.57	−0.62
	0.5	−1.33	−1.65	−1.91	−1.20	−1.42	−1.74
R_d	1.5	2.49	2.49	2.49			
	0.5	1.50	1.50	1.50			
K_d	1.5	−1.65	−1.70	−1.72	−1.65	−1.72	−1.72
	0.5	−4.94	−11.30	−68.73	−4.29	−8.48	−46.69
B_d	1.5	−0.08	−0.10	−0.08	−0.20	−0.26	−0.19
	0.5	−0.09	−0.11	−0.08	−0.24	−0.34	−0.25
ΔT (piscivore)	1.5				−0.63	−0.61	−0.63
	0.5				−1.78	−1.69	−1.80
C (*M. muelleri*)	1.5				0.91	0.87	0.91
	0.5				0.96	0.94	0.96

Figure 2. (a) Surface irradiance (PAR, ln-transformed) recorded on 2 November 2007; (b) vertical temperature (T), light extinction coefficient (*K*), plankton density (D) and estimated plankton size (R) profiles; (c) acoustic echogram from 2 November 2007 showing pearlside sound scattering layers (SSL1, SSL2 and SSL3) in the upper 200 m (the *y*-axis scale is the same as for the environmental variables); (d) estimated ambient light intensity at upper and lower SSL depths. Time is UTC (local Norwegian time – 1 h). In the echogram, numbers correspond to approximate depth and time of multisampler trawl stations shown in Table 1.

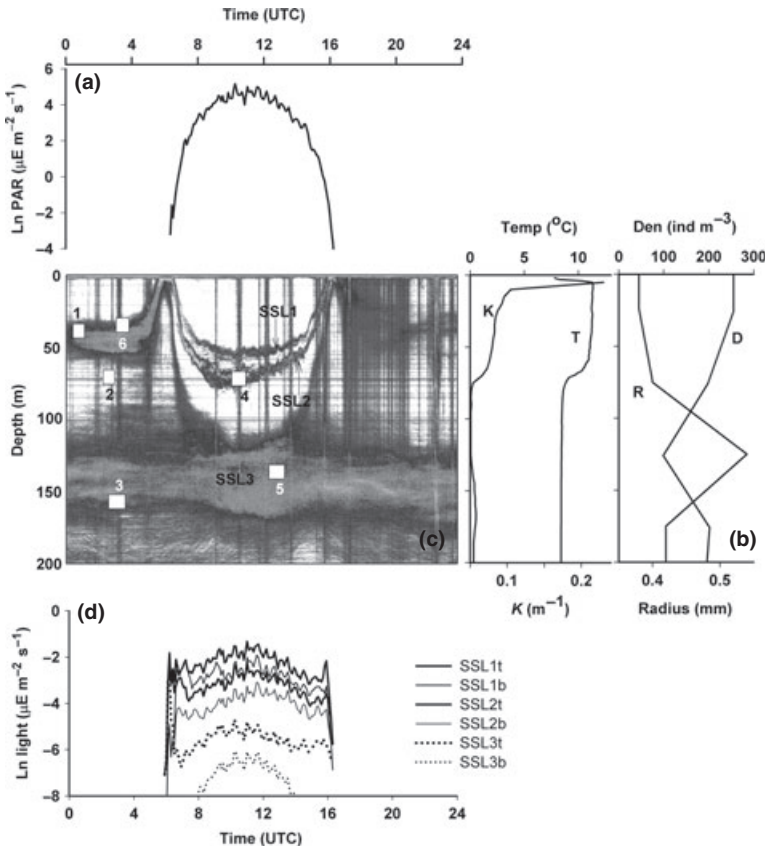

Temperature (Fig. 2b) at the surface was about 7.8°C and increased rapidly to 11.4°C at 9 m depth. There was a marked thermocline between 60 and 75 m. Here temperature dropped from 11 to 8.5°C and remained relatively constant throughout deeper depth. The estimated diffuse light attenuation K_d decreased most visibly in the upper 15–20 m, decreasing further gradually down to 70 m before remaining stable at about 0.05 m^{-1}.

Generally, high numbers of copepods were found throughout the water column, but somewhat higher densities of copepods occurred in the upper 50 m. Figure 2b displays vertical distribution of zooplankton abundance (individuals m^{-3}) and individual radius (mm) (estimated from dry mass) from a multinet haul taken at 09:40 h.

Migration patterns of SSLs

Three SSLs were visible on the acoustic echogram at day: SSL1 at 50–60 m, SSL2 at 66–80 m, and SSL3 at 110–165 m (Fig. 2c). Fish from SSL1 and SSL2 displayed crepuscular DVM, ascending at 14:00 h (UTC) and reaching the surface 20 min after sunset, at 16:00 h (UTC). Fish descended the next day to their daytime depths approximately 36 min before sunrise, at 06:28 h (UTC), (Fig. 2c), at which point surface irradiance was 0.3 μE m^{-2} s^{-1}. The large majority of pearlside from SSL3 remained at constant deeper depths throughout the entire diel period. Only a seemingly small proportion of fish from SSL3 migrated to the surface at dusk, and also between midnight and dawn (Fig. 2c). At dawn, fish that returned to SSL3 started their descent before fish from SSL1 and SSL2 (Fig. 2c).

Ambient light intensities in scattering layers

The three SSLs experienced different light intensities (Fig. 2d) due to different vertical positions. The light intensity at the upper and lower edges of each SSL remained fairly constant throughout the light period

(Fig. 2d). Midday light intensities at the bottom and top of SSLs ranged from 0.06 to 0.11 μE m^{-2} s^{-1} in SSL1, 0.02–0.4 μE m^{-2} s^{-1} in SSL2 and from 0.0006 to 0.005 μE m^{-2} s^{-1} in SSL3. Fish at the top of SSL1 and SSL2 thus experienced 8–20 times higher light intensities than SSL3 fish, whereas fish at the bottom of SSL1 and SSL2 had 30–100 times more light than corresponding fish in SSL3. At dawn in particular, light intensities in SSL1 and SSL2 were 20–60 times higher than at SSL3 depth (Fig. 2d).

Feeding and vertical length distribution

Numerically copepods were the dominant food item in pearlside stomachs. Of the 423 stomachs analysed, only two contained euphausiids, one amphipods, and nine fish eggs, while the remaining stomachs contained just copepods. The percentage of fish with empty stomachs, i.e., number of ingested copepods, varied greatly between stations and as such with fish size (Table 1). Fish caught above 50 m between midnight and dawn covered a broad length range (20–40 mm; Fig. 3a) and had fewer prey items in their stomachs (average 10 copepods; Fig. 3b) than juveniles from SSL2 (24 mm; Fig. 3a station 4) caught at day at 80 m depth (average 49 copepods; Fig. 3b). Adult fish from SSL3 averaged 39 mm in length (Fig. 3a) and generally had fewer copepods in their stomachs (Fig. 3b) but the percentage of fish with empty stomachs was much lower at day (43%) than at night (94%; Table 1; Fig. 3b), suggesting limited daytime feeding. Copepods identified in pearlside stomachs were less digested in day samples than in night-time samples (Fig. 3c). Based on trawl catches from a field campaign in Masfjorden in 2008, which identified the shallowest SSL1 as pearlside post-larvae (Staby *et al.*, 2011), we assumed that post-larvae with a similar size (10 mm) as in 2008 constituted SSL1 in 2007.

Zooplankton encounter rate

Calculated weight-specific zooplankton encounter rates (Eqn 5) are displayed in Figure 4a. During light hours, pearlside in SSL1 experienced the highest encounter rates (0.11 g g^{-1} h^{-1}), followed by SSL2 (0.036 g g^{-1} h^{-1}) and SSL3 (0.014 g g^{-1} h^{-1}). SSL1 fish experienced relatively high encounter rates throughout the daytime with a maximum around noon and local peaks at dawn and dusk, whereas juveniles in SSL2 and migrating SSL3 adults had a maximum encounter rate at dawn and relatively stable but lower encounter rates during daytime and dusk. The daily copepod encounter rates calculated for juvenile fish in the upper (61) and lower (26) part of SSL2 and adult fish in the upper (27) and lower (4) non-migrating part of SSL3 were within the range of copepods identified in the fish stomach samples (Fig. 3b) from the corresponding layers.

Predation rate

The predation rates calculated for the three SSLs (Eqn 6; Fig. 4b) show that throughout the light period, fish from SSL2 and SSL3 (the ones at the surface at dawn) are susceptible to the highest predation rate (3.2×10^{-4} h^{-1}), followed by SSL1 (1.12×10^{-4} h^{-1}). The non-migrating adults in SSL3 experience a very low mortality rate, with a maximum of 2.6×10^{-5} h^{-1}. The daily variations in predation rates resemble those of zooplankton encounter rates.

Figure 3. (a) Standard length, (b) number of ingested copepods and (c) degree of copepod digestion in *Maurolicus muelleri* sampled at different depths and times of day (numbers in the left graph correspond to trawl stations shown in Fig. 2c, where the open circles correspond to day stations 4 (at SSL2 depth) and 5 (at SSL3 depth), and dark squares to night stations 1, 2, 3 and 6. Bars from left to right show 1 SD, maximum number of copepods in an individual fish, and 25–75 percentiles of ranked observations. In the scale for digestion, zero denotes undigested prey and one unrecognizable prey.

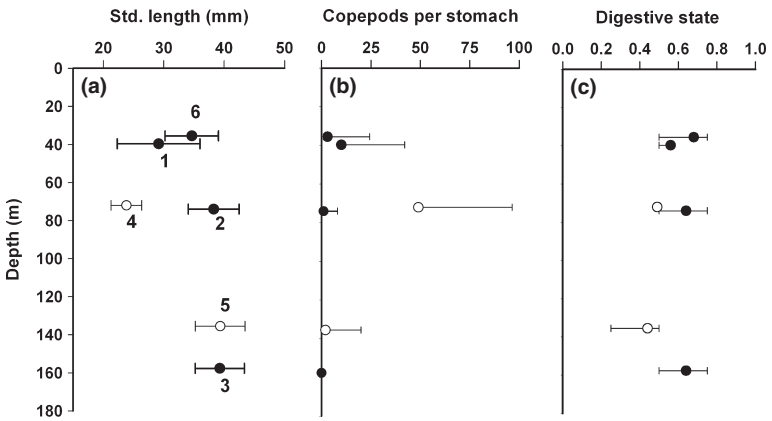

Figure 4. Model estimates of (a) zooplankton encounter rates (E_w per unit fish mass, g g^{-1} h^{-1}), (b) visual mortality rates M (h^{-1}) and (c) M/E_w ratio (g g^{-1}) of visual mortality rate over mass specific zooplankton encounter rate, for the top (t) and bottom (b) edge of *Maurolicus muelleri* sound scattering layers (SSL).

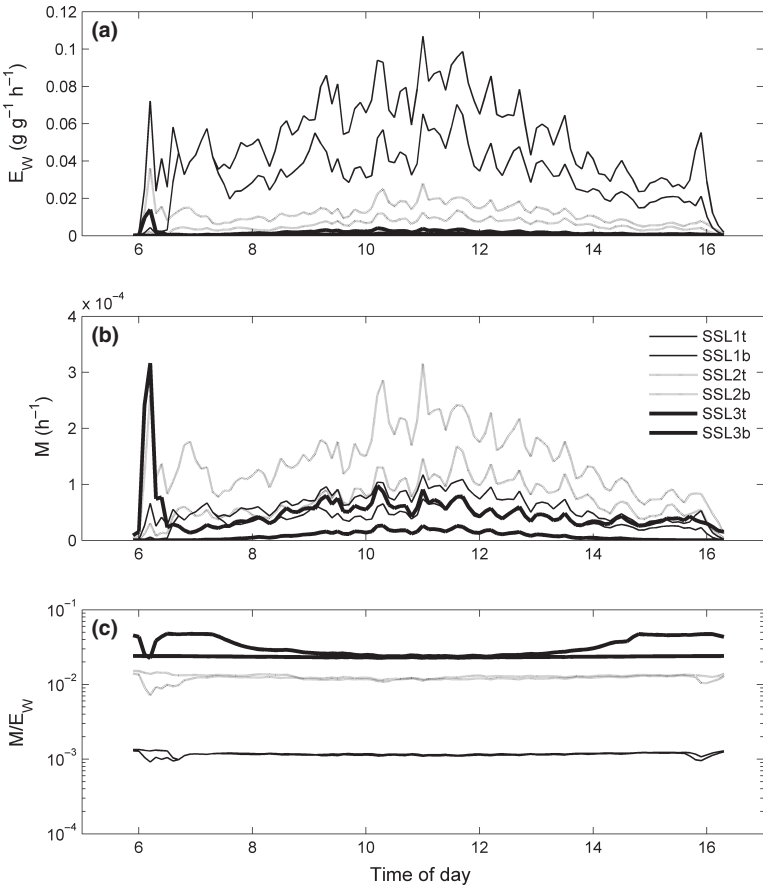

Mortality over feeding ratio

The ratios between predation (M, Eqn 6) and prey encounter rates (E_w, Eqn 5) are displayed in Figure 4c. The M/E_W ratio for post-larvae in SSL1 is less than for juveniles in SSL2 and adults SSL3. The M/E_W ratios in SSL1 and SSL2 are quite constant during daytime, but drop during dawn and dusk for the upper part of the layers. The M/E_W ratio in the upper part of SSL3 increases during dawn and dusk, except for a drop in the early part of the dawn period.

The vertical profiles of weight-specific zooplankton encounter rates for the three fish sizes are displayed by the solid lines for a noon situation in Figure 5a. Decreasing light intensity with depth is the most effective variable, but depth profiles in zooplankton size and density also interrupt the exponential light function between 70 and 175 m, while light saturation (on the fish retina) limits the increase in visual range in the upper 50-m interval.

The vertical profiles of visual predation risk over mass specific encounter rates for the three fish sizes are displayed by the solid lines for a noon situation in Figure 5b. Here the relative effects of zooplankton abundance and size are more pronounced, as the calculated predation rate does not incorporate vertical density gradients in M. *muelleri*. The effect of water turbidity is also evident in the upper 10 m, where the M/E_w ratio drops rapidly since the 'long-sighted' piscivore predators are relatively more affected by the turbid water than the 'short-sighted' M. *muelleri*. The stabilization of the M/E_w ratio occurring in the last 2 m is caused by light saturation in both planktivore and piscivore fish.

The dashed and dotted lines in both diagrams show the effects of changing the half-saturation coefficient (k_l) for light and the diffuse light extinction coefficient (K_d), respectively, from the sensitivity runs (Table 3).

Figure 5. (a) Vertical profiles of prey encounter rate (*Ew*) and (b) visual mortality over prey encounter rate (*M*/*Ew*) in the standard run (solid lines) and for changes in the eye half-saturation constant (k_I) (dashed solid lines) and for changes in the diffuse light attenuation coefficient (K_d) (dotted lines). The profiles represent the situation at noon with maximum daylight.

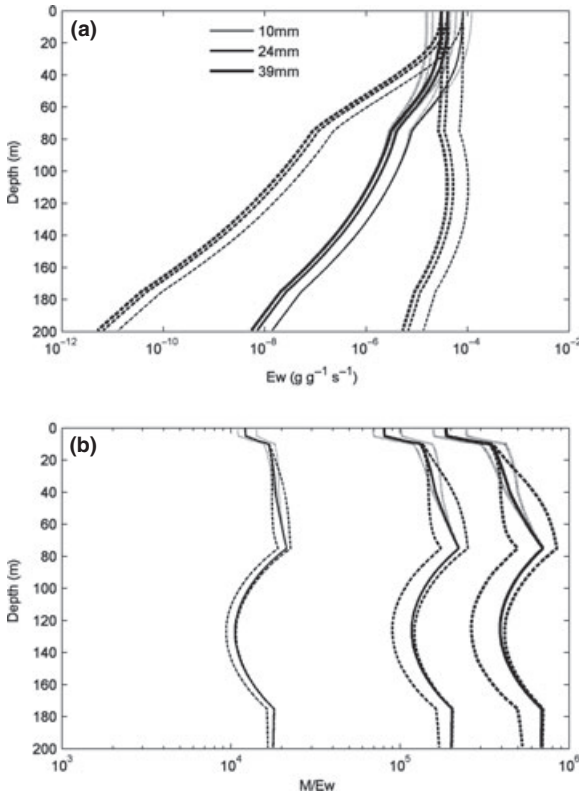

Sensitivity analysis

The sensitivity analysis (Table 3) shows that most of the parameters have a sensitivity index (S) in the absolute range [0.5–2.5], which classifies as More sensitive (S > 0.4) according to Wei *et al.* (2004). The exception is the beam attenuation coefficient (b_d), which induces an Insensitive (S < 0.1) response to visual prey encounter rate (E_w), while Sensitive (0.1 < S < 0.4) response to the visual predation rate on *M. muelleri*. Changes in the diffuse light attenuation coefficient (K_d) induce a strong response in the model which increases from SSL1 to SSL3. An important issue with respect to our research objectives is how parameters and environmental variables influence the vertical differences between the SSLs. The sensitivity analysis shows that the SSLs respond similarly to most parameters except for the diffuse light attenuation (K_d), which causes different responses in each SSL. The reason for this is that the light attenuation will have a cumulative and exponential effect on light intensity with increasing depth and thus have a stronger impact on prey encounters and visual mortality (Fig. 5, dotted lines) for fish at deep locations (SSL3). A reduction in the half-saturation coefficient for light (k_I) also produces different responses in the SSLs because it only becomes effective in the brighter water masses where SSL1 and SSL2 are located (Fig. 5, dashed lines).

DISCUSSION

The difference in DVM behaviour, i.e., habitat selection, of juvenile and adult pearlside observed in late autumn is in accordance with findings from previous studies (Giske *et al.*, 1990; Baliño and Aksnes, 1993; Bjelland, 1995; Kaartvedt *et al.*, 2008). Different ontogenetic stages of pearlside seem to adopt different trade-off strategies between growth and survival (Giske and Aksnes, 1992; Rosland and Giske, 1994; Rosland, 1997). Post-larvae and juvenile fish maintain high feeding rates of copepods by selecting a fairly constant light environment during DVM (Staby and Aksnes, 2011) and also experience a reduced M/E_W ratio in the turbid surface waters at dawn and dusk. The large proportion of non-migrating adult fish, on the other hand, choose to distribute deeper at day and not migrate to the surface towards dusk, thereby minimizing predation risk and forsaking high zooplankton encounter rates.

The size and species composition of SSLs restricted to the upper 250 m in Masfjorden have been described thoroughly in previous studies (Kaartvedt *et al.*, 1988; Giske *et al.*, 1990; Baliño and Aksnes, 1993; Rasmussen and Giske, 1994; Bagøien *et al.*, 2001; Staby *et al.*, 2011), and show that (i) pearlside dominate the species composition, and (ii) smaller fish constitute shallower SSLs. Length at maturity (L_{50}) estimates indicate that pearlside become mature at a length of 24–30 mm (Rasmussen and Giske, 1994; Bjelland, 1995), implying that SSL2 was mainly composed of immature juveniles and SSL3 of adult fish, which is consistent with earlier studies.

Our findings corroborate results from previous studies that pearlside feed at day time, and that in autumn, as in winter months, fish feed mainly on copepods (Giske *et al.*, 1990; Bagøien *et al.*, 2001). At night, stomach fullness was lower and digestion of identifiable prey more advanced than at day before noon (Fig. 3c). However, the average number of captured copepods found in this study was much higher than in any of the previous studies (Giske *et al.*, 1990; Bagøien *et al.*, 2001), indicating vertical differences in seasonal

and interannual abundance and availability of copepods. The number of copepods pearlside consumed was regardless of SSL similar to the models of prey encounter estimates. This suggests that the model estimates for prey encounters are likely to be underestimates, as not every encounter results in a successful capture and ingestion.

Selecting a shallower and brighter environment should increase both the probability of detecting zooplankton and being predated on by pelagic piscivorous fish. Calculated zooplankton encounter rates (Fig. 4a) confirm this assumption, with the largest growth potential found in the shallowest SSL1, followed by SSL2 and the deepest SSL3. The same tendency is also seen within each SSL, and fish in the upper positions of the SSL experience larger growth potential than those in the deeper end (Fig. 4a). However, calculated visual predation rates (Fig. 4b) deviate from the vertical profiles in light intensity, and fish in SSL1, in spite of their shallower distribution, are actually less susceptible to visual predation than fish in SSL2. The explanation for this is that the small size of post-larvae fish in SSL1 makes them less susceptible to visual predation than their larger juvenile conspecifics in SSL2, in spite of the higher light intensity in SSL1. The sensitivity analysis also demonstrated a relatively strong sensitivity to prey radius (Table 3). Other factors such as transparency of the post-larvae could actually increase this effect, but we have not included that effect in the model due to lack of data to parameterize it.

Different trade-offs between growth and survival may be explained by ontogenetic and state-dependent differences (Giske and Aksnes, 1992; Rosland and Giske, 1994; Rosland, 1997), but as suggested here the size dependency in visual foraging and predation may affect how the trade-off rules are translated into DVM strategies. Mortality rate over weight-specific prey encounter rate (M/E_W ratio) reflects the instantaneous trade-off between survival and growth (Werner and Gilliam, 1984; Giske and Aksnes, 1992). The model suggests that post-larvae in SSL1 can prioritize higher growth at a lower cost of visual predation (Fig. 4c) than larger fish in SSL2 and SSL3. The larger juveniles in SSL2 also prioritize high growth but may have to pay a higher cost of visual predation as a consequence of this.

The M/E_W ratios in SSL1 and SSL2 are at a minimum during the crepuscular periods (Fig. 4c) because of the turbid surface water conditions and higher beam attenuation (contrast reduction), which inhibits the reaction distances of piscivore predators relatively more than that of the planktivore *M. muelleri*. Thus the contrast reduction occurring in the turbid surface waters may represent an additional mechanism (i.e., low M/E_w ratio) to the anti-predation window (Clark and Levy, 1988; Rosland and Giske, 1994; Kaartvedt *et al.*, 1998) at dawn and dusk. The M/E_W ratio for non-migrating fish (SSL3) was constant throughout the diel cycle, whereas migrating adult fish from SSL3 experienced an increasing M/E_W ratio during their descent and ascent (Fig. 4c), suggesting a higher predation risk by piscivores associated with their vertical relocation. Migrating adults seemingly only benefit from the higher surface turbidity for a short period at dawn. However, stomach content analysis indicated that the large majority of adult fish had not captured any copepods at dusk (Fig. 3b), implying that the potential feeding-related gain associated with DVM is small for migrating SSL3 fish.

Stomach fullness may also be an important physiological factor that is not accounted for here. After several hours of night darkness the fish probably have a high feeding motivation (hunger level) and empty stomachs at dawn, which enables them to utilize the feeding opportunity at dawn to a maximum.

Previous studies showed that adult fish start normal DVM to the surface after winter in spring (Rasmussen and Giske, 1994; Bjelland, 1995; Goodson *et al.*, 1995; Staby *et al.*, 2011). This indicates a seasonal switch in the M/E_W rule in combination with seasonal changes in the vertical habitat structure. Autumn and winter months in Norwegian fjords are generally characterized by low primary production and a vertical distribution of zooplankton, where the larger individuals are located in deeper positions (Bagøien *et al.*, 2001). Less turbid water combined with relatively lower prey profitability at the surface could thus trigger an adult non-migrating strategy during late autumn and winter in Norwegian fjords with emphasis on predator avoidance.

The model for visual range (Aksnes and Utne, 1997) has been set up with simplifying assumptions about the target organisms (fish and zooplankton) being spherical and with similar contrast properties. Differences in shape and coloration within and between zooplankton species, and between ontogenetic stages of the pearlside, will influence the visual ranges of pearlside and its predators. Variation in transparency, degree of silvering and possibly also counter-illumination between ontogenetic stages may also influence pearlside susceptibility to visual predation (Warrant and Locket, 2004).

The model is sensitive to parameters and environmental variables, which is not unexpected since the model is merely based on one equation (Eqn 2), which gives a direct relationship between model parameters

and the simulated variable. Since we focus on the relative differences between SSLs, the model sensitivity in terms of changes in the absolute values was not important here as long as the changes were consistent in all SSLs. However, non-linear process in the light attenuation and light saturation of the eye could change the vertical ratios between the different SSLs as demonstrated in Figure 5 and Table 3.

We have only considered the visual processes in foraging and predation risk, but other factors related to state and condition (Hays *et al.*, 2001; Pearre, 2003) and physiological processes (Wurtsbaugh and Neverman, 1988; Giske *et al.*, 1990; Bevelhimer and Adams, 1993) may also influence DVM behaviour. In some zooplankton species, migration may be state-dependent, well fed individuals with large energy reserves being more likely to refrain from migrating to the surface compared with starved animals (Forward and Hettler, 1992; Hays *et al.*, 2001). Whereas the large fraction of adult fish in SSL3 does not perform DVM, prioritising a low predation risk environment, a small proportion of adult fish disobeys this strategy and ascends to the surface before dawn and at dusk. Prior to ceasing DVM, non-migrating adults enhance their condition and build up sufficient lipid deposits in summer months (Falk-Petersen *et al.*, 1986; Hulley and Prosch, 1987), which enables them to survive at depth during winter periods with reduced feeding opportunities. In contrast, migrating adults may be in an impaired condition or have insufficient energy reserves, requiring them to migrate to the surface layer to feed, but exposing them to an increasing predation risk. We found that some adults from the shallower stations (>30 mm SL) had a lower condition factor than non-ascending adults, but the trend was not consistent for all the stations. Additional analysis of the size-dependent state and condition-related DVM variability is therefore required. Shortly after dusk, fish at the surface descended to deeper depths (midnight sinking), constituting the night-time scattering layer positioned above the thermocline at 70–80 m. Such nocturnal descents may result from avoidance of shallow distributed piscivores predators (Staby, 2010), or the selection of growth optimizing temperatures (Giske *et al.*, 1990). While juvenile pearlside and probably also post-larvae remained above the thermocline at night at temperatures >11°C (but well below the colder surface layer of <8°C), increasing growth rates by maximizing available time in the warm water layer, most large adult fish in SSL3 stayed in the colder water (<8°C) below 125 m during both day and night to reduce metabolic costs and energy losses at low feeding rates (Giske *et al.*, 1990).

ACKNOWLEDGEMENTS

We thank Stein Kaartvedt and Anders Røstad for making available acoustic data and assisting with acoustic data processing, Mette Hordnes for providing AFDW data, and the crew and students onboard the RV *Håkon Mosby*.

REFERENCES

Aksnes, D.L. and Utne, A.C.W. (1997) A revised model of visual range in fish. *Sarsia* **82:**137–147.

Aksnes, D.L., Dupont, N., Staby, A., Fiksen, Ø., Kaartvedt, S. and Aure, J. (2009) Coastal water darkening and implications for mesopelagic regime shifts in Norwegian fjords. *Mar. Ecol. Prog. Ser.* **387:**39–49.

Bagøien, E., Kaartvedt, S., Aksnes, D.L. and Eiane, K. (2001) Vertical distribution and mortality of overwintering *Calanus*. *Limnol. Oceanogr.* **46:**1494–1510.

Baliño, B. and Aksnes, D.L. (1993) Winter distribution and migration of the sound scattering layers, zooplankton and micronekton in Masfjorden, western Norway. *Mar. Ecol. Prog. Ser.* **102:**35–50.

Bevelhimer, M.S. and Adams, S.M. (1993) A bioenergetics analysis of diel vertical migration by Kokanee salmon, *Oncorhynchus nerka*. *Can. J. Fish. Aquat. Sci.* **50:** 2336–2349.

Bjelland, O. (1995) Life history tactics of two fjordic populations of *Maurolicus muelleri*. Cand. scient. thesis, University of Bergen. pp. 79.

Clark, C.W. and Levy, D.A. (1988) Diel vertical migrations by juvenile sockeye salmon and the antipredation window. *Am. Nat.* **131:**271–290.

Cohen, J.H. and Forward, R.B. (2009) Zooplankton diel vertical migration – a review of proximate control. *Oceanogr. Mar. Biol.* **47:**77–110.

De Robertis, A. (2002) Size-dependent visual predation risk and the timing of vertical migration: an optimization model. *Limnol. Oceanogr.* **47:**925–933.

Eggers, D.M. (1978) Limnetic feeding behavior of juvenile sockeye salmon in Lake Washington and predator avoidance. *Limnol. Oceanogr.* **23:**1114–1125.

Engås, A., Skeide, R. and West, C.W. (1997) The 'MultiSampler': a system for remotely opening and closing multiple codends on a sampling trawl. *Fish. Res.* **29:** 295–298.

Falk-Petersen, I.-B., Falk-Petersen, S. and Sargent, J.R. (1986) Nature, origin and possible roles of lipid deposits in *Maurolicus muelleri* (Gmelin) and *Benthosema glaciale* (Reinhart) from Ullsfjorden, northern Norway. *Polar Biol.* **5:**535–540.

Forward, R.B. Jr and Hettler, W.F. (1992) Effects of feeding and predator exposure on photoresponses during diel vertical migration of brine shrimp larvae. *Limnol. Oceanogr.* **37:** 1261–1270.

Giske, J. and Aksnes, D.L. (1992) Ontogeny, season and trade-offs: vertical distribution of the mesopelagic fish *Maurolicus muelleri*. *Sarsia* **77:**253–261.

Giske, J., Aksnes, D.L., Baliño, B. *et al.* (1990) Vertical destribution and trophical interactions of zooplankton and fish in Masfjorden, Norway. *Sarsia* **75:**65–81.

Giske, J., Aksnes, D.L. and Fiksen, Ø. (1994) Visual predators, environmental variables and zooplankton mortality risk. *Vie Millieu* **44:**1–9.

Gjøsæter, J. (1981) Life history and ecology of *Maurolicus muelleri* (Gonostomatidae) in the Norwegian waters. *Fiskeridirektoratets Skrifter, Serie Havundersøkelser* **17:**109–131.

Gjøsæter, J. and Kawaguchi, K. (1980) A review of the world resources of mesopelagic fish. *FAO Fisheries Technical Paper* **193:** 1–151.

Goodson, M.S., Giske, J. and Rosland, R. (1995) Growth and ovarian development of *Maurolicus muelleri* during spring. *Mar. Biol.* **124:**185–195.

Grand, T.C. (1999) Risk-taking behaviour and the timing of life history events: consequences of body size and season. *Oikos* **85:**467–480.

Hays, G.C., Kennedy, H. and Frost, B.W. (2001) Individual variability in diel vertical migration of a marine copepod: why some individuals remain at depth when others migrate. *Limnol. Oceanogr.* **46:**2050–2054.

Houston, A.I., McNamara, J.M. and Hutchinson, J.M.C. (1993) General results concerning the trade-off between gaining energy and avaoiding predators. *Philos. Trans. R. Soc. Lond. B.* **341:**375–397.

Hrabik, T., Jensen, P.P., Martell, S.J.D., Walters, C.J. and Kitchell, J.F. (2006) Diel vertical migration in the Lake Superior pelagic community. I. Changes in the vertical migration of coregonids in response to varying predation risk. *Can. J. Fish. Aquat. Sci.* **63:**2286–2295.

Hulley, P.A. and Prosch, R.M. (1987) Mesopelagic fish derivatives in the southern Benguela upwelling region. *S. Afr. J. Mar. Sci.* **5:**597–611.

Johnsen, S. and Sosik, H.M. (2003) Cryptic coloration and mirrored sides as camouflage strategies in near-surface pelagic habitats: implications for foraging and predator avoidance. *Limnol. Oceanogr.* **48:**1277–1288.

Kaartvedt, S., Aksnes, D.L. and Aadnesen, A. (1988) Winter distribution of macroplankton and micronekton in Masfjorden, western Norway. *Mar. Ecol. Prog. Ser.* **45:**45–55.

Kaartvedt, S., Knutsen, T. and Holst, J.C. (1998) Schooling of the vertically migrating mesopelagic fish *Maurolicus muelleri* in light summer nights. *Mar. Ecol. Prog. Ser.* **170:**287–290.

Kaartvedt, S., Torgersen, T., Klevjer, T., Røstad, A. and Devine, J.A. (2008) Behaviour of individual mesopelagic fish in acoustic scattering layers of Norwegian fjords. *Mar. Ecol. Prog. Ser.* **360:**201–209.

Kaartvedt, S., Røstad, A., Klevjer, T. and Staby, A. (2009) Use of bottom-mounted echo sounders in exploring behavior of mesopelagic fishes. *Mar. Ecol. Prog. Ser.* **395:**109–118.

Lima, S.L. and Dill, L.M. (1990) Behavioral decisions made under the risk of predation: a review and prospectus. *Can. J. Zool.* **68:**619–640.

Neilson, J.D. and Perry, R.I. (1990) Diel vertical migrations of marine fishes: an obligate or facultative process? *Adv. Mar. Biol.* **26:**115–168.

Parin, N.V. and Kobyliansky, S.G. (1996) Diagnosis and distribution of fifteen species recognized in genus *Maurolicus* cocco (Sternoptichydae, Stomiiformes) with a key to their identification. *Cybium* **20:**185–195.

Pearre, S. Jr (2003) Eat and run? The hunger/satiation hypothesis in vertical migration: history, evidence and consequences *Biol. Rev.* **78:**1–79.

Rasmussen, O.I. and Giske, J. (1994) Life-history parameters and vertical distribution of *Maurolicus muelleri* in Masfjorden in summer. *Mar. Biol.* **120:**649–664.

Rosland, R. (1997) Optimal responses to environmental and physiological constraints: evaluation of a model for a planktivore. *Sarsia* **82:**113–128.

Rosland, R. and Giske, J. (1994) A dynamic optimization model of the diel vertical distribution of a pelagic planktivorous fish. *Progr. Oceangr.* **34:**1–43.

Ryer, C.H. and Olla, B.L. (1999) Light-induced changes in the prey consumption and behaviour of two juvenile planktivorous fish. *Mar. Ecol. Prog. Ser.* **181:**41–51.

Scheuerell, M.D. and Schindler, D.E. (2003) Diel vertical migration by juvenile sockeye salmon: empirical evidence for the antipredation window. *Ecology* **84:**1713–1720.

Staby, A. (2010) Seasonal dynamics in the vertical migration behaviour of mesopelagic fish. PhD thesis, University of Bergen, pp. 126.

Staby, A. and Aksnes, D. (2011) Follow the light – diurnal and seasonal variation in vertical distribution of the mesopelagic fish *Maurolicus muelleri*. *Mar. Ecol. Prog. Ser.* **422:**265–273.

Staby, A., Kaartvedt, S. and Røstad, A. (2011) Long-term acoustical observations of the mesopelagic fish *Maurolicus muelleri* reveal novel and varied vertical migration patterns. *Mar. Ecol. Prog. Ser.* **441:**441–455.

Utne-Palm, A.C. (2002) Visual feeding of fish in a turbid environment: physical and behavioural aspects. *Mar. Fresh. Behav. Physiol.* **35:**111–128.

Vogel, J.L. and Beauchamp, D.A. (1999) Effects of light, prey size, and turbidity on reaction distances of lake trout (*Salvelinus namaycush*) to salmonid prey. *Can. J. Fish. Aquat. Sci.* **56:**1293–1297.

Warrant, E.J. and Locket, N.A. (2004) *Biol. Rev. Camb. Philos. Soc.* **79:**671–712.

Wei, H., Sun, J., Moll, A. and Zhao, L. (2004) Phytoplankton dynamics in the Bohai Sea – observations and modelling. *J. Mar. Sys.* **44:**233–251.

Werner, E.E. and Gilliam, J.F. (1984) The ontogenetic niche and species interactions in size-structured populations. *Annu. Rev. Ecol. Syst.* **15:**393–425.

Widder, E.A. (1999) Bioluminescence. In: Adaptive mechanisms in the ecology of Vision. S.N. Archer, M.B.A. Djamgoz, E.R. Loew & J.C. Partridge (eds). Dordrecht: Kluwer Academic Publishers, pp. 555–581.

Wurtsbaugh, W.A. and Neverman, D. (1988) Post-feeding thermotaxis and daily vertical migration in a larval fish. *Nature* **333:**846–848.